An Embedded Dual-Band Base Station Antenna Array Employing Choked Bowl-Shaped Antenna for Cross-Band Scattering Mitigation

Yi He[1], Can Ding[1], Gengming Wei[1], Y. Jay Guo[1]
[1] Global Big Data Technologies Centre, University of Technology Sydney (UTS), Ultimo, NSW, Australia
e-mail address: Yi.He@student.uts.edu.au

***Abstract*—An embedded dual-band dual-polarized base station antenna (BSA) array is proposed in this paper. The array consists of two low-scattering bowl-shaped antenna elements working at the lower band (LB) and five cross-dipoles operating at the higher band (HB). Such an array configuration is intended to mitigate the negative effect on the HB antennas' radiation pattern caused by the presence of adjacent LB antennas. In this paper, a new LB antenna loaded with metal chokes is proposed to further reduce its scattering to the HB radiation. The results obtained with conventional bowl-shaped LB antenna and with choked LB antenna are compared to demonstrate the superiority of this de-scattering method. The simulation results show that the HB performance is significantly improved with the help of metal chokes while the LB performance remains nearly unchanged.**

***Index Terms*—Base station antenna (BSA), bowl-shaped element, dual-band, dual-polarization, embedded scheme, metal choke, scattering mitigation.**

I. INTRODUCTION

As a key component of mobile communication systems, base station antennas (BSAs) have received considerable attention in the past decades. The complex communication environment and the growing demand for high-speed, high-quality signal transmission pose stringent requirements on the BSAs. They generally need to have dual-polarization operation, stable half-power beamwidth, low cross-polarization levels, wide frequency bandwidth, etc. [1]. On the other hand, in order to achieve maximum utilization of space resources and reduce the maintenance costs of antenna systems, BSAs covering different frequency bands are collocated on the same platform with close proximity. For example, a widely-used 4G BSA array usually holds two different antennas covering the bands of 698-960 MHz and 1710-2690 MHz, respectively [2, 3]. To enable both 4G and 5G operation on the same compact antenna panel, additional antennas operating at sub-6 GHz, e.g., 3.3-3.8 GHz, would also need to be integrated with the 4G antennas [4], which leads to a more complicated electromagnetic environment. The close placement of the antennas in different frequency bands causes severe cross-band interference that will deteriorate antenna performance, especially higher band (HB) elements' radiation pattern.

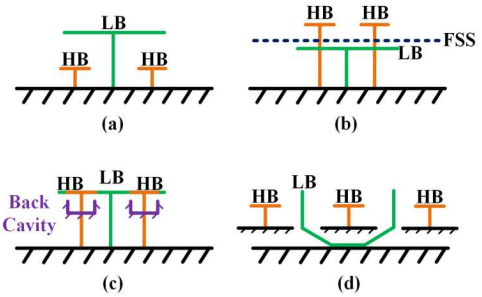

Fig. 1. Four dual-band array arrangements for base station application. (a) HB beneath LB. (b) HB above LB. (c) HB and LB share the same aperture. (d) HB inside LB.

As illustrated in Fig. 1, there are several types of array arrangements to accommodate two kinds of antennas working in different bands on the same panel for base station applications. The most convenient and widely used configuration is the side-by-side arrangement with the HB elements placed under the LB elements, as shown in Fig. 1(a). The LB antennas having larger size serve as big scatterers for the HB radiation, which can greatly deteriorate the radiation performance of the HB elements. In our previous works [5, 6], lumped and distributed chokes serving as low-pass high-stop filters are inserted to the LB antennas, which makes the LB has a significantly reduced scattering performance. Together with an array topology optimization [7], the cross-band scattering issue can be solved.

Fig. 1(b) shows another array configuration with HB antennas located on top of LB antennas and an FSS layer is inserted in between [8, 9]. In this configuration, the LB antenna will not block the HB radiation. Moreover, the isolation between the two bands is improved by the FSS layer functioning as a reflector for HB radiators. The drawback of this configuration is the relatively lower gain of the LB antennas and the complex structure that increases the manufacturing and assembly costs.

As depicted in Fig. 1(c), one could also design a single aperture shared by both LB and HB radiators [10]. The back cavity is used as a reflector for the HB element, which also alleviates the adverse effect on HB performance from LB. However, since the HB element is embedded into the gap of the LB's loop arm, the inner diameter of the loop limits the size of the HB radiator, which makes this arrangement only applicable to the case where the two bands are far apart from each other.

The last arrangement is to employ bowl-shaped LB antennas and place some HB elements inside the LB antennas [11-13], as shown in Fig. 1(d). This embedded scheme naturally has less cross-band interacting problem for the HB element placed inside the LB but the performance of the HB elements outside the LB antennas remain to be an issue.

The second and third arrangements illustrated in Figs. 1(b) and 1(c) are new and they haven't been really used in industrial products yet. The first and the last configurations shown in Figs. 1(a) and 1(d), on the other hand, are quite mature. While there are several cross-band scattering mitigation works based on the side-by-side scheme, no one has tried to improve the performance of the embedded scheme. Besides, all the available works currently suffers from relatively narrower scattering suppression bandwidth, i.e., the "invisibility" of the LB antennas is only valid for a narrower bandwidth at the HB. Therefore, this cross-band scattering issue in dual-band BSA has not been fully solved yet.

In this paper, based on the embedded scheme, a new bowl-shaped LB antenna is developed. Metal chokes based on the choking technique proposed in our previous work [5] are redesigned to fit with the bowl-shaped antenna and they are inserted to both the radiators and the baluns, leading to an excellent scattering suppression performance. Compared to [5], significant bandwidth enhancement has been achieved. Compared to the conventional dual-band BSA array based on the embedded scheme, the radiation performance deterioration caused by the cross-band scattering is greatly alleviated.

II. Array Configuration

A. Array Arrangement and HB Element

The proposed dual-band dual-polarized BSA array consists of two bowl-shaped LB elements and five HB elements in an embedded interlaced arrangement, as illustrated in Fig. 2. The element spacing of the LB array and HB array is 0.68 λ_{LB} and 0.91 λ_{HB}, respectively, where λ_{LB} and λ_{HB} represent the wavelength at the center frequency of the corresponding working bands. The widely used cross-dipole is chosen as the HB radiator, which comprises two pairs of mutually perpendicular conductor arms, two baluns, two feeding bridges, and a box-reflector [1, 14, 15].

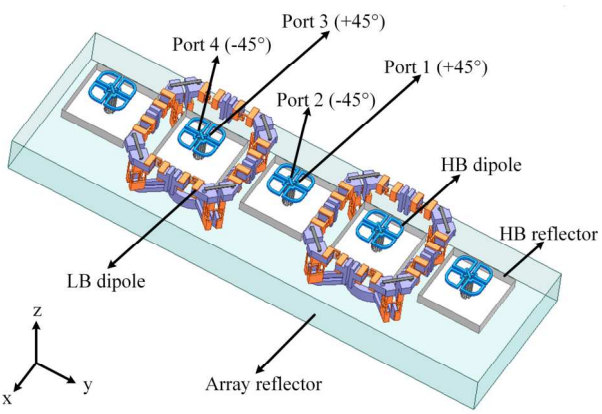

Fig. 2. The proposed dual-band dual-polarized BSA array based on embedded scheme.

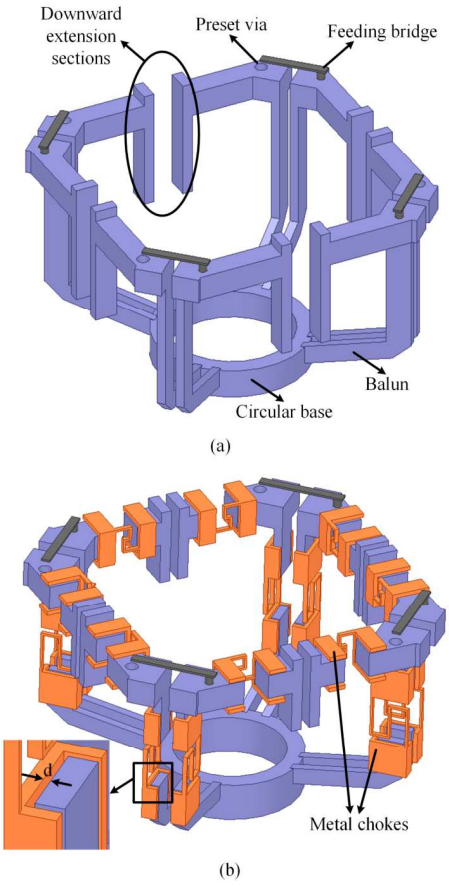

Fig. 3. The configuration of the (a) conventional and (b) choked bowl-shape LB antenna.

B. LB Element

As presented in Fig. 3(a), the conventional LB bowl-shaped element includes four identical dipoles sharing the same circular base. Adjacent dipoles are tightly coupled with the help of additional downward extension sections to expand the operating bandwidth. A pair of diagonal-located two dipoles radiate with the same polarization, i.e., either

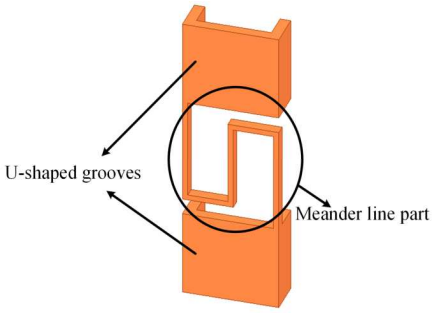

Fig. 4. The configuration of the metal choke.

+45° or -45°. By exciting the two pair of dipoles separately, dual-orthogonal polarizations can be obtained.

Each dipole consists of a balun, a feeding bridge, and four metal chokes. The balun has a vertical section and an inclined section, and the upper and lower ends are connected to the corresponding radiation arms and the grounded circular base, respectively. The outer conductor of the coaxial cable is attached to one arm of the dipole through the preset via, while the inner conductor is extended to the other arm by the feeding bridge.

Based on the conventional LB bowl-shaped element, in this work, the LB antenna (both the dipole arms and the baluns) is truncated into short parts whose electrical lengths are all less than the half-wavelength at 2.7 GHz (the highest frequency at HB) to make the LB element electromagnetically "invisible" to the HB antenna, as shown in Fig. 3(b). Then the short segments are reconnected by metal chokes functioning as low-pass high-stop filters to enable the LB operation. The partial enlarged detail in Fig. 3(b) illustrates that the metal choke is capacitively coupled to (rather than directly connected to) the antennas with a small distance of d = 1 mm. The size of the choked LB bowl-shaped element is $0.43\lambda_{LB}$*$0.43\lambda_{LB}$*$0.26\lambda_{LB}$, where λ_{LB} represents the free-space wavelength at the center frequency of LB (0.825 GHz).

C. *Metal Choke*

The metal chokes used in this work has a similar working principle as the one proposed in [5] but they are implemented differently to fit with the antenna structure. Fig. 4 gives a more detailed schematic of the metal choke. The choke is composed of a meander line and two U-grooves. The S-shaped meander line has a thickness of 2 mm and works as a parallel resonance filter in HB, which can be equivalent to a capacitor and an inductor in parallel [16]. By adjusting the size of the meander line to change the inductance and capacitance of the parallel resonance, the induced current on the LB element can be minimized and kept at a very low level in HB, thus reducing the impact on HB radiation. Although the presence of the meander line creates a large series inductance for LB operation, a broadband impedance matching can still be achieved by adding series capacitance as a reactance compensation through the U-grooves with a small distance from the radiation arm.

Once the induced current on LB dipole arm is optimized for the lowest level in the target frequency band, the size of

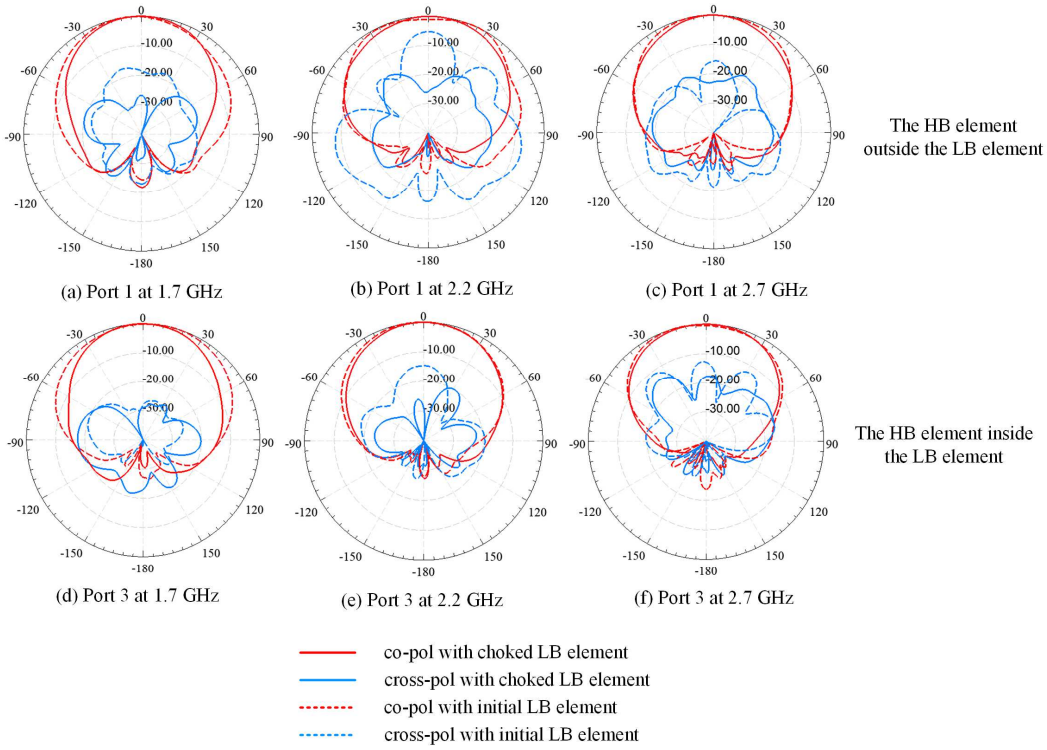

Fig. 5. Simulated co- and cross-pol radiation patterns of the HB elements in the *xoz*-plane

TABLE I. HPBW OF HIGH BAND ELEMENTS (°)

Frequency (GHz)	Port 1		Port 3	
	Conventional LB	*Choked LB*	*Conventional LB choke*	*Choked LB*
1.7	78.44	63.98	91.91	72.45
2.2	94.27	72.19	62.83	64.13
2.7	69.92	60.59	74.94	70.50

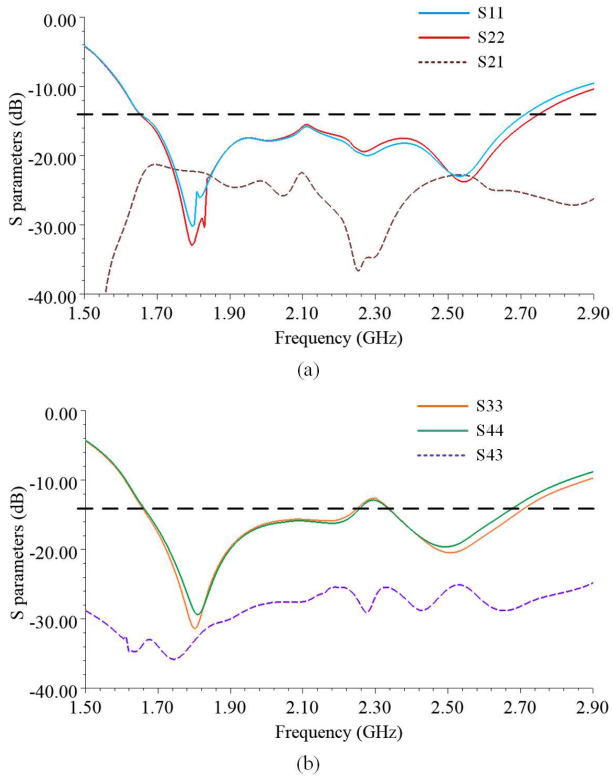

Fig. 6. Simulated S parameters of HB elements (a) outside and (b) inside the LB element.

the meander part is fixed. Then by changing the relative parameters of the U-grooves, the coupling capacitance can be adjusted to counteract the large inductance brought by the meander part. Furthermore, the metal chokes are also added on the baluns as they also pose a negative effect on HB dipoles. Adjusting the parameters of the two sets of chokes yields better outcomes compared to the initial array employing conventional LB antennas. The final version of the LB element and the supporting structures for the metal chokes can be subsequently determined.

III. SIMULATION RESULTS

By replacing the conventional bowl-shaped LB antenna elements with the choked one, the performance of the HB element can be enhanced. Note that the performance improvements for the HB elements inside and outside the LB elements are different. Due to the symmetry of the two polarizations, we only show the performance of one polarization, i.e., the results obtained by exciting ports 1 and

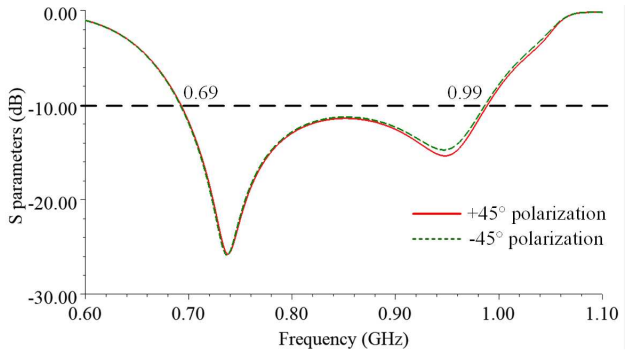

Fig. 7. Simulated S parameters of the LB element.

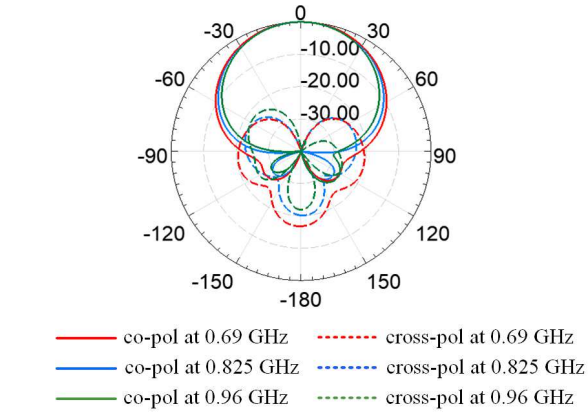

Fig. 8. Simulated co- and cross-pol radiation patterns of the LB element in the *xoz*-plane.

3. As shown in Fig. 2, ports 1 and 3 refer to the ports of HB elements located outside and inside the LB elements, respectively.

Fig. 5 compares the simulation results of the normalized HB radiation patterns in the *xoz*-plane of the HB antennas located inside and outside the LB element at three typical frequency points, before and after inserting the metal chokes to the LB elements. As shown in the figure, even with the initial LB element, the pattern distortion is not that obvious, which is attributed to the embedded array arrangement. However, with the presence of conventional LB element, the cross-polarization level is very high, especially for the HB antenna located outside of the LB element. This is generally not acceptable for base station applications [17, 18]. With the choked LB elements, the cross-polarization radiation is remarkably suppressed.

Moreover, Table I compares the HPBW of the two HB antennas when the conventional and choked bowl-shaped LB antennas are presented. It can be concluded that the patterns of HB elements (both the elements inside and outside of the LB antenna) are much more stable after loading the metal chokes.

As depicted in Fig. 6, the HB elements outside and inside the LB element can both provide –14 dB impedance bandwidths of 47.7% in the upper band, ranging from 1.66 to 2.7 GHz. The isolations between the two polarizations of the two HB elements are > 21 dB and 25 dB, respectively.

Fig. 7 shows the reflection coefficients of LB element in ±45° polarizations. The results of the two ports are quite similar due to symmetry, which can both provide –10 dB impedance bandwidths of 35.7% from 0.69 to 0.99 GHz. Fig. 8 shows the simulated normalized radiation patterns at 0.69, 0.825, and 0.96 GHz of one polarization for the LB element in the *xoz*-plane. The HPBW varies within 63°±4°, which means that stable patterns have been achieved in LB. The simulated realized gain is from 8.4-9.9 dBi, indicating that the chokes introduce minor losses to the LB.

IV. CONCLUSION

A dual-band dual-polarized BSA array was presented in this paper. The array consists of two LB elements operating at 0.69-0.99 GHz and five HB elements covering the band of 1.66-2.7 GHz. This array utilizes an embedded configuration, i.e., some HB antennas are enclosed by LB antennas, to mitigate the pattern distortion to the HB element due to the close proximity of adjacent antennas. Moreover, metal chokes functioning as low-pass high-stop filters were inserted to the LB antennas' radiating arms and baluns, which significantly reduced the LB antennas' scattering at the HB. Despite the chokes' negative effects on impedance matching, the LB antennas were successfully matched across a wide frequency bandwidth. By replacing the conventional bowl-shaped LB antenna with the choked one, the radiation performance was noticeably improved in terms of cross-polarization level and stability.

REFERENCES

[1] C. Ding, H. Sun, R. W. Ziolkowski, and Y. J. Guo, "Simplified Tightly-Coupled Cross-Dipole Arrangement for Base Station Applications," IEEE Access, vol. 5, pp. 27491-27503, 2017.

[2] H. Huang, Y. Liu, and S. Gong, "A Dual-Broadband, Dual-Polarized Base Station Antenna for 2G/3G/4G Applications," IEEE Antennas and Wireless Propagation Letters, vol. 16, pp. 1111-1114, 2017.

[3] R. Wu and Q. X. Chu, "A Compact, Dual-Polarized Multiband Array for 2G/3G/4G Base Stations," IEEE Transactions on Antennas and Propagation, vol. 67, no. 4, pp. 2298-2304, 2019.

[4] G. N. Zhou, B. H. Sun, Q. Y. Liang, S. T. Wu, Y. H. Yang, and Y. M. Cai, "Triband Dual-Polarized Shared-Aperture Antenna for 2G/3G/4G/5G Base Station Applications," IEEE Transactions on Antennas and Propagation, vol. 69, no. 1, pp. 97-108, 2021.

[5] H. Sun, C. Ding, H. Zhu, B. Jones, and Y. J. Guo, "Suppression of Cross-Band Scattering in Multiband Antenna Arrays," IEEE Transactions on Antennas and Propagation, vol. 67, no. 4, pp. 2379-2389, 2019.

[6] H. Sun, H. Zhu, C. Ding, B. Jones, and Y. J. Guo, "Scattering Suppression in a 4G and 5G Base Station Antenna Array Using Spiral Chokes," IEEE Antennas and Wireless Propagation Letters, vol. 19, no. 10, pp. 1818-1822, 2020.

[7] Y. Xiong, C. Ding, Z. Cheng, and Y. J. Guo, "Cross-Band Interaction Mitigation in Dual-Band Antenna Arrays for 4G/5G and Beyond," in 2021 15th European Conference on Antennas and Propagation (EuCAP), 2021, pp. 1-5.

[8] Y. Chen, J. Zhao, and S. Yang, "A Novel Stacked Antenna Configuration and its Applications in Dual-Band Shared-Aperture Base Station Antenna Array Designs," IEEE Transactions on Antennas and Propagation, vol. 67, no. 12, pp. 7234-7241, 2019.

[9] Y. Zhu, Y. Chen, and S. Yang, "Decoupling and Low-Profile Design of Dual-Band Dual-Polarized Base Station Antennas Using Frequency-Selective Surface," IEEE Transactions on Antennas and Propagation, vol. 67, no. 8, pp. 5272-5281, 2019.

[10] Y. Li and Q. X. Chu, "Coplanar Dual-Band Base Station Antenna Array Using Concept of Cavity-Backed Antennas," IEEE Transactions on Antennas and Propagation, pp. 1-1, 2021.

[11] Y. He, Z. Pan, X. Cheng, Y. He, J. Qiao, and M. M. Tentzeris, "A Novel Dual-Band, Dual-Polarized, Miniaturized and Low-Profile Base Station Antenna," IEEE Transactions on Antennas and Propagation, vol. 63, no. 12, pp. 5399-5408, 2015.

[12] H. Huang, Y. Liu, and S. Gong, "A Novel Dual-Broadband and Dual-Polarized Antenna for 2G/3G/LTE Base Stations," IEEE Transactions on Antennas and Propagation, vol. 64, no. 9, pp. 4113-4118, 2016.

[13] Y. He, W. Tian, and L. Zhang, "A Novel Dual-Broadband Dual-Polarized Electrical Downtilt Base Station Antenna for 2G/3G Applications," IEEE Access, vol. 5, pp. 15241-15249, 2017.

[14] H. Sun, H. Zhu, C. Ding, and Y. J. Guo, "Wideband Planarized Dual-Linearly-Polarized Dipole Antenna and Its Integration for Dual-Circularly-Polarized Radiation," IEEE Antennas and Wireless Propagation Letters, vol. 17, no. 12, pp. 2289-2293, 2018.

[15] Z. Bao, Z. Nie, and X. Zong, "A Novel Broadband Dual-Polarization Antenna Utilizing Strong Mutual Coupling," IEEE Transactions on Antennas and Propagation, vol. 62, no. 1, pp. 450-454, 2014.

[16] F. Losee, RF Systems, Components, and Circuits Handbook, Second Edition. Artech, 2005.

[17] C. Ding, H. Sun, R. W. Ziolkowski, and Y. J. Guo, "A Dual Layered Loop Array Antenna for Base Stations With Enhanced Cross-Polarization Discrimination," IEEE Transactions on Antennas and Propagation, vol. 66, no. 12, pp. 6975-6985, 2018.

[18] Y. Luo, Q. Chu, and D. Wen, "A Plus/Minus 45 Degree Dual-Polarized Base-Station Antenna With Enhanced Cross-Polarization Discrimination via Addition of Four Parasitic Elements Placed in a Square Contour," IEEE Transactions on Antennas and Propagation, vol. 64, no. 4, pp. 1514-1519, 2016.